Environmental Pollution 379 (2025) 126542

Contents lists available at ScienceDirect

Environmental Pollution

journal homepage: www.elsevier.com/locate/envpol

Macrophages-derived exosomal non-coding RNA circ_0055194 regulating miR-665/YAP1/Twist axis is involved in pulmonary fibrosis induced by Nd_2O_3 ☆

Yuanqi He [1], Yuhang Zhao [1], Kai Wu, Danyan Qi, Yupeng Ma, Wenjie Li, Xiangyu Chang, Suhua Wang *, Yanrong Gao **

School of Public Health, Baotou Medical College, Baotou, 014040, Inner Mongolia, PR China

ARTICLE INFO

Keywords:
Neodymium oxide (Nd_2O_3)
Extracellular vesicle
Macrophage-differentiated THP-1 cells
Fibroblast activation
Pulmonary fibrosis

ABSTRACT

Globally, rare earth elements (REEs) have found extensive applications, and the occupational and environmental health concerns they pose have garnered significant attention. Neodymium oxide (Nd_2O_3) is widely extracted and processed as a raw material. However, there is a paucity of research on the mechanisms underlying Nd_2O_3-induced lung fibrosis. In this study, we first discovered that the non-coding RNA circ_0055194 levels were elevated in the serum of patients with rare earth pneumoconiosis(REP), and we observed that mice exposed to Nd_2O_3 resulted in lung damage and fibrosis, which were associated with elevated levels of mmu_circ_0013556 (homologous to human hsa_circ_0055194), Yes-associated protein 1 (YAP1), Twist, and α-smooth muscle actin (α-SMA), along with decreased levels of miR-665. Additionally, in human embryonic lung fibroblasts (HELF) co-cultured with macrophages exposed to Nd_2O_3, increased circ_0055194 levels and decreased miR-665 levels facilitated the activation of YAP1/Twist axis, fibroblast proliferation, transformation, and extracellular matrix (ECM) expression. Further investigation revealed a significant elevation in the expression of circ_0055194 in macrophage-derived exosomes upon Nd_2O_3 exposure, and these exosomal circ_0055194 targeted miR-665 in HELF cells, as confirmed by pull-down experiments demonstrating the adsorption of miR-665 by circ_0055194. Inhibition of circ_0055194 in macrophages or overexpression of miR-665 resulted in decreased expression of YAP1 and Twist in HELF cells, along with reduced ECM components (collagenI, α-SMA), the binding of miR-665 to 3′UTR of YAP1mRNA was verified through luciferase reporter gene experiments. Moreover, in mice, CRISPR-Cas9-mediated knockout of the circ_0013556 gene reversed miR-665 levels and Nd_2O_3-induced lung fibrosis, and suppressed the level of the YAP1 and Twist. In conclusion, this study demonstrates that exosomal circ_0055194, by sponging miR-665 to regulate YAP1 facilitating Twist expression, participates in Nd_2O_3-induced pulmonary fibrosis, representing one of the mechanisms lung fibrosis caused by Nd_2O_3 exposure. This information suggests that exosomal circ_0055194 could serve as a biomarker for Nd_2O_3-induced pulmonary fibrosis.

1. Introduction

With the extensive utilization of rare earth elements (REEs) in diverse industrial applications, growing concerns have emerged regarding their environmental and occupational health implications. Inhalation represents the primary exposure route for rare earth particles, with prolonged exposure triggering a pathogenic progression from inflammatory lesions to fibrotic proliferation in pulmonary tissues, ultimately culminating in pneumoconiosis development (Gwenzi et al., 2018; Lian et al., 2022). Rare earth pneumoconiosis (REP) has consequently emerged as a significant global health challenge. The pathogenesis of REP involves complex molecular pathways, particularly the

☆ This paper has been recommended for acceptance by Wen Chen.

* Corresponding author. The Key Laboratory of Modern Toxicology of Baotou Medical College, School of Public Health, Baotou Medical College, Baotou, 014040, Inner Mongolia, PR China.

** Corresponding author. The Key Laboratory of Modern Toxicology of Baotou Medical College, School of Public Health, Baotou Medical College, Baotou, 014040, Inner Mongolia, PR China.

E-mail addresses: bt_wangsuhua@163.com (S. Wang), 15047211335@163.com (Y. Gao).

[1] Authors contributed equally.

https://doi.org/10.1016/j.envpol.2025.126542
Received 12 February 2025; Received in revised form 23 May 2025; Accepted 25 May 2025
Available online 26 May 2025

pulmonary toxicity mechanisms induced by Nd_2O_3 nanoparticles, which remain incompletely characterized (Chen et al., 2003; Bu et al., 2022). Our studies have demonstrated that Nd_2O_3 exposure induces sustained inflammatory responses and alveolar epithelial damage in murine models, culminating in progressive pulmonary fibrosis (Chen et al., 2003; Bu et al., 2023). However, comprehensive elucidation of the molecular cascades underlying Nd_2O_3-induced pathogenesis requires further mechanistic investigation through advanced experimental approaches.

Studies indicated that the proliferation and transformation of fibroblasts into myofibroblasts(FMT) contribute to the accumulation of extracellular matrix (ECM), ultimately resulting in pulmonary fibrosis due to environmental and occupational hazards. However, researches indicated that particles, such as silica, which caused pneumoconiosis, did not directly impact the cytoactive properties and differentiation of fibroblast (Wang et al., 2020; Youet al., 2023). Thus, the process of FMT is regulated indirectly by other cells and signaling molecules. Exosomes (Exos) serve as critical mediators of intercellular communication, carrying a diverse cargo of biomolecules—including proteins, lipids, nucleic acids, and glycosylated complexes—that play a role in the pathogenesis of pulmonary fibrosis (Conigliaro and Cicchini, 2018; You et al., 2023). Alveolar macrophages and fibroblasts play crucial roles in the pathogenesis of pneumoconiosis. Exosomes from macrophages exposed to SiO_2 (SiO_2-Exos) are pro-fibrotic, exacerbating pulmonary fibrosis and inflammation during pneumoconiosis. Inhibiting exosomes production can suppress lung inflammation and alleviate PF (Yang et al., 2022). Our previous study have shown that co-culture of macrophages exposed to Nd_2O_3 with fibroblasts induced macrophage M2 polarization to facilitate fibroblast proliferation and FMT (Bu et al., 2023). However, the mechanism by which macrophages influence fibroblasts in rare earth-induced pulmonary fibrosis remains to be elucidated.

Non-coding RNAs (ncRNAs) are widely implicated in various diseases such as cancer, immunodeficiency, neurodegenerative diseases, aging, and cardiovascular diseases, moreover, circRNAs also play crucial roles in pulmonary fibrosis (Mannaertset al., 2015; Zhouet al., 2020; Kishore and Petrek, 2021). The unique and more stable structure of circRNAs, along with their resistance to RNase R, makes them highly competitive as biomarkers and therapeutic targets (Jeck and Sharpless, 2014). In our previous research, by profiling the ncRNA expression in the plasma of REP patients (Shiet al., 2021). In previous studies, we found that after Nd_2O_3 exposure, lncRNA H19/miR-29a-3p/SNIP1/c-myc pathway was activated, accelerated macrophage M2 polarization, and led to lung tissue fibrosis in mice(Bu et al., 2023). We found multiple ncRNA with differential expression in the serum exosomes of patients with REP(Gaoet al., 2025). Based on bioinformatics and statistical analysis, we proposed that circ_0055194 may be significantly related to the onset and progression of REP. Elucidating the relationship between circ_0055194 and Nd_2O_3 induced pulmonary fibrosis is therefore critical to improving our understanding of this disease.

In this study, we screened for abnormally expressed circ_0055194 and predicted through the database website (https://circinteractome.nia.nih.gov/) that circ_0055194 could serve as a molecular sponge for miR-665, with miR-665 regulating the expression of YAP1 (https://mirdb.org/). Macrophages exposed to Nd_2O_3 induce the secretion of exosomes, and fibroblasts were co-cultured with macrophages exposed or not exposed to Nd_2O_3. These results demonstrate that circ_0055194 is secreted by macrophages exposed to Nd_2O_3 and transfers to fibroblasts via exosomes after co-culture, acting as a molecular sponge to down-regulate miR-665, activates the YAP1/Twist signaling pathway, promotes the proliferation of fibroblasts and their differentiation into myofibroblasts, leading to excessive ECM deposition.

2. Materials and methods

2.1. Study subjects and Biospecimen Collection

Thirty-six patients diagnosed with REP in a rare earth smelting plant from 2016 to 2020 were selected as the REP group, while thirty-six healthy individuals with participants in the physical examinations were chosen as control group. The REP group was non-smokers, aged 53.26 ± 4.71 years. The control group were non-smokers with no history of dust exposure and no significant abnormalities on DR chest X-ray. All subjects were male and no other pulmonary or bronchial diseases were found. Age and length of service were compared between the two groups. The circRNA profiles from the serum exosomes of 9 REP patients (divide into three groups) and 9 healthy individuals by random sampling from a total of study subjects, including 36 REP patients and 36 healthy individuals, were detected by high-throughput RNA sequencing, the relevant methods have been previously delineated in our earlier work (Gao et al., 2025). The study was approved by the Medical Ethics Committee of Baotou Medical College and informed consent was obtained from all patients.

2.2. Rare earth Nd_2O_3 particles treatment

In the present study, the Nd_2O_3 particles employed in animal trials were characterized by an irregular polyhedral morphology, with a mean dynamic diameter of roughly 60 nm. Upon exposure to RPMI-1640, these particles exhibited an average hydrodynamic size of 540.20 nm and a zeta potential of 4.26 mV. The physicochemical properties of these Nd_2O_3 particles have been previously delineated in our earlier work (Bu et al., 2022). For the cellular assays, a stock solution was prepared by dissolving 5 mg of Nd_2O_3 in 5 mL of sterile phosphate-buffered saline (PBS), which was then serially diluted to achieve concentrations of 0, 6.25, 12.5, and 25 μg/mL using RPMI-1640. The Nd_2O_3 particles were subjected to autoclaving at 103.4 kPa (1.05 kg/cm^2) and 121 °C for 20 min in an autoclave (Esco Enterprise Development, Shanghai). They were then placed in an electrothermal constant temperature blast drying oven (Anhe Zhengheng Instrument, Sichuan) at 60 °C overnight for use in subsequent animal experiments conducted in a dynamic nose-only inhalation exposure chamber (HOPE-MED 8050H, Tianjin).

2.3. Mouse treatment

Six-to eight-week-old male C57BL/6J mice were obtained from Sibef (Beijing) and allowed to adapt at the Baotou Medical College. The experimental protocol was approved by the Ethics Committee for Experimental Animals at Baotou Medical College. This investigation was undertaken to elucidate the impact of Nd_2O_3 on lung injury. Mice were positioned in a dynamic nose-inhalation exposure chamber using a supporting device, with their noses and mouths directed towards the rare earth dust generator with different concentrations (0, 500, 1000, 2000 mg/m^3) of Nd_2O_3 in the dynamic exposure chamber for 2 h on one day,then harvested 7, 28 or 56 days later. Age-matched mice, housed in a comparable environment but without any exposure to Nd_2O_3, were used as the control group.

To determine whether circ_0013556 (homologous to human hsa_circ_0055194) is involved in Nd_2O_3-induced pulmonary fibrosis in mice, mice were tracheal instillated with 0.1 ml ml of circ_0013556 gRNA(or sh-NC) gene AAV9 adenovirus suspension and 0.1 ml of DIO-spCAS9 gene AAV9 adenovirus suspension in AAV9-sh-circ_0013556 group. Mice in the AAV9-sh-circ_0013556 group, AAV9-sh-NC group, and Nd_2O_3 group (6–8 weeks old) were positioned in a dynamic nose-inhalation exposure chamber using a supporting device, with their noses and mouths directed towards the rare earth dust generator with 2000 mg/m^3 Nd_2O_3 in the dynamic exposure chamber for 7,28,56 days, 2 h on one day.

2.4. Cell culture

The THP-1 cell lineage, representative of human macrophages and originating from a case of acute monocytic leukemia (source: Procell Life Sciences, Wuhan), was cultivated in RPMI-1640 medium augmented with 10 % fetal bovine serum (FBS, from Thermo Fisher Scientific, USA), as well as antibiotics including streptomycin (100 mg/mL) and penicillin (100 U/mL), in an environment of 5 % CO_2and37 °C. For experimental protocols, THP-1 cells underwent a transformation into adherent macrophages (designated THP-M) following a 24-h incubation with (100 ng/mL) phorbol ester (PMA). Additionally, human embryonic lung fibroblasts (HELF cells, a specific cell line that is generally available and has passed ethical review provided, provided by Qingqi Biotechnology Development, Shanghai) were cultured in DMEM (Invitrogen, Carlsbad, CA, USA) supplemented with identical concentrations of FBS and antibiotics, under the same atmospheric conditions. The propagation of both cell types involved a bi-daily subculture routine, with a division ratio of 1:3.

2.5. Lung histopathology

The lung tissues of the mice were first fixed in a 4 % paraformaldehyde solution to preserve their structural integrity, followed by embedding in paraffin to facilitate sectioning. For histological examination and to assess the extent of collagen deposition, 5 μm-thick sections of the lung tissue were carefully mounted onto slides. These sections were then stained using both hematoxylin and eosin (H&E) for general tissue morphology, and Masson's trichrome to specifically highlight collagen fibers. Following staining, the sections were quantified for histological features using ImageJ software for measurement and analysis.

2.6. Immunohistochemistry

The Tissue samples of the lung were initially fixed in formalin to preserve their morphological integrity, followed by a thorough dehydration process using anhydrous ethanol. The samples were then carefully embedded in paraffin, sectioned into thin slices, and affixed onto glass slides. These slides were subsequently dried and baked to guarantee firm adhesion.Prior to immunohistochemical staining, the samples underwent a rehydration step using 85 % and 75 % ethanol for precise durations, followed by a thorough rinse with double-distilled water to remove any residual reagents.To effectively suppress the activity of endogenous peroxidase, the tissue sections were subjected to a treatment process involving immersion in a 3 % hydrogen peroxide (H_2O_2) solution for a duration of 20 min, all while maintaining a constant temperature of 25 °C to ensure optimal reaction conditions. Following PBS buffer washes to eliminate unbound reagents, non-specific binding was minimized by blocking the sections with 5 % bovine serum albumin at 37 °C for 40 min. Finally, eight typical areas were chosen at random from each section for thorough inspection and captured using high-resolution imaging with an optical microscope. The expression level of the target protein was carefully assessed based on the staining intensity and quantitatively analyzed using a semi-quantitative H-score method.

2.7. RNA pull-down assay

HELF cells were lysed in a buffer containing a specific cocktail of reagents, including 20 mM Tris (pH 7.5), 200 mM NaCl, 2.5 mM $MgCl_2$, 0.05 % Igepal, 60 U/mL Superase-In, 1 mM dithiothreitol, and protease inhibitors. After centrifugation, the supernatant was collected, with a 50-μl aliquot retained for future analysis. The remaining supernatant was mixed with biotin-labeled miR-665 or a negative control, incubated at room temperature for 2 h, and then incubated with magnetic beads for 1 h. After magnetic separation, total RNA was extracted and determined by qRT-PCR.

2.8. Luciferase reporter assays

To explore the impact of miR-665 on the 3′UTR of YAP1, we cloned sequences harboring either the wild-type or a mutated version of the miR-665 seed sequence into the psiCHECK-2 vector at the *Xho*I and *Not*I restriction enzyme sites (provided by GENEray, China). These constructs were named psiCH-YAP1-WT and psiCH-YAP1-MUT, respectively. HEK 293 cells, grown to 70–80 % confluency, were co-transfected with these luciferase reporter plasmids along with miR-665 mimics or a negative control mimic (miR-NC) utilizing Lipofectamine 2000 (from Thermo Fisher Scientific, USA). After a 48-h incubation period, the cells were harvested, and luciferase activity was assessed using the Dual-Luciferase Reporter Assay System from Promega (USA) on a TECAN Infinite M200 PRO multimode microplate reader (Switzerland). The Renilla luciferase signal was employed as an internal reference to normalize for variations in transfection efficiency.

2.9. Quantitative real-time PCR

RNA was extracted from cultured mouse lung tissue, THP-M cells, and HELF cells using Trizol reagent (Thermo Fisher Scientific, USA). Subsequently, 1 μg of the extracted RNA was converted into cDNA using the PrimeScript RT kit from Vazyme Biotech (China). For real-time quantitative polymerase chain reaction (qRT-PCR), the GoTaq® qPCR Master Mix kit from Promega was utilized, and fluorescent signals were monitored using a QuantStudio 5 qPCR system from Thermo Fisher Scientific. The primers used in this study were custom-synthesized by Qingdao Biotechnology Co., Ltd. Table 1. The relative expression of the target genes was calculated using the $2^{-\Delta Ct}$ method and normalized to the expression levels of U6 (used for mice), and glyceraldehyde-3-phosphate dehydrogenase (GAPDH, used for human cells).

2.10. RNA interference

Custom-synthesized by GenePharma (Shanghai), the sequences included those targeting hsa_circ_0055194 for small interfering RNA (siRNA) knockdown, a control siRNA featuring a scrambled sequence, an inhibitor specific to miR-665, and a negative control miRNA. Transfection of PMA-THP-M cells was executed using lip2000, adhering to the manufacturer's instructions. Adenoviral vectors (AAV9-sh-circ_0013556) and the corresponding nonsense sequence were synthesized by Shandong Vigene Biosciences (Jinan, China) to knockdown mmu_circ_0013556.

2.11. Western blot analysis

For immunoblotting and immunoprecipitation studies, proteins were isolated from HELF cells and lung tissue. Cell lysates were prepared using a protease inhibitor cocktail (Beyotime) supplemented with 1 mM PMSF, while animal tissues were homogenized in RIPA buffer (also from Beyotime). Protein concentrations were determined using the Pierce™ BCA Protein Assay Kit (Thermo Fisher Scientific), following the manufacturer's instructions. After separation by SDS-PAGE, the proteins were

Table 1
Primer sequences employed.

	Sequences
hsa_circ_0055194	F:ATCAGCCTCTTCCCGCAAAT
	R:GTGAAGGCTTGGTCGCATTG
mmu_ circ_0013556	F:CCTACCTGTGCATAGCCTCG
	R:AGAAGACAGTGGATGCCAGC
miR-665	F:ATTATACCAGGAGGCTGAGGCC
U6	F:CTCGCTTCGGCAGCACATATACT
	R:ACGCTTCACGAATTTGCGTGTC
GAPDH	F:TCGTGGAGTCTACTGGCGTCTT
	R:CATTGCTGACAATCTTGAGGGAG

transferred onto PVDF membranes (Millipore, USA) and subsequently blocked with QuickBlock solution (Beyotime) for 1 h. The membranes were then incubated with specific primary antibodies at 4 °C overnight. Following washes with TBST, the membranes were probed with a goat anti-rabbit secondary antibody at a dilution of 1:50,000 for 1 h at room temperature. The protein bands were detected using Odyssey CLX infrared imaging system, the band intensity was quantitatively assessed using ImageJ software, and normalized with GAPDH.

2.12. Exosome extraction

The supernatant of THP-M cells was collected via ultra-high-speed centrifugation. Initially, the samples were centrifuged at 3000×*g* for 10 min to eliminate cellular debris, followed by centrifugation at 2000×*g* for 20 min to remove dead cells. Subsequently, pre-treated samples were subjected to centrifugation at 10,000×*g* at 4 °C for 30 min to further deplete impurities such as residual cellular debris and large granular proteins. The supernatant was then collected and ultra-centrifuged at 100,000×*g* for 70 min at 4 °C. The supernatant was discarded, and the resulting pellet was resuspended in PBS. This pellet was re-centrifuged at 100,000×*g* for 70 min at 4 °C, with the supernatant being discarded and the process repeated 2–3 times to ensure purity. Finally, the pellet was resuspended in an appropriate volume of PBS or buffer solution, yielding the extracted exosomes.

The identification of cell-derived exosomes is the basis for ensuring the purity and functional research of exosomes. Its core methods include observing morphological characteristics by transmission electron microscopy (TEM) and detecting membrane protein markers (CD9, CD63, CD81, TSG101) by Western blot.

2.13. ZetaView nanoparticle tracker

The particle size distribution of exosomes was quantitatively analyzed using a ZetaView nanoparticle tracking system.Firstly, dilute the exosome sample 10,000-fold with 1xPBS and store it on ice for subsequent analysis.Secondly, clean the detection chamber with double-distilled water, ensuring complete removal of any air bubbles. Finally, using a syringe, inject the prepared sample into the detection chamber. Set the frame rate to 30 frames per second to initiate detection, and subsequently generate the particle size distribution profile of exosomes.

2.14. Statistical analysis

In this work, data were shown as mean ± SD. GraphPad 6.0 software was used to carry out all the statistical analyses. The normality of the distribution was checked by Shapiro-Wilk test. Comparison between several groups or two groups among was performed via one-way ANOVA or Student's t-test. Any difference with P-value <0.05 was deemed significant in statistics.

3. Results

3.1. Non-coding RNA profiling of serum exosomes from REP patients revealed a significant upregulation of circ_0055194, and expression levels of circ_0055194 were elevated in serum exosomes in an expanded cohort of REP patients

We collected serum exosome samples from REP patients and healthy individuals for high-throughput RNA sequencing and analyzed differences in non-coding RNA expression (Gao et al., 2025). At the same time, among the differentially expressed circRNAs, we selected those with significant changes for bioinformatics analysis to clarify their functions. Through RNA sequencing (Three patients) and qRT-PCR (Thirty-six patients) detection, the expression level of circ_0055194 in serum exosomes of REP patients was significantly increased (Fig. 1A and B).

3.2. The circ_0013556 expression was increased, miR-665 level was decreased, and the YAP1/Twist signaling pathway was activated in Nd_2O_3-induced lung tissue fibrosis of mice

Previous prediction results from the database website showed that circ-0055194 can bind miR-655, and miR-655 can target YAP1. So, we've done a preliminary confirmation in vivo. Researches have found that YAP1 serves as a crucial effector in the Hippo pathway. The overexpression of YAP1 enhances the transcriptional activation of Twist, thereby facilitating cell proliferation, migration, and collagen synthesis in lung fibroblasts through interaction with TEAD (Chen et al., 2019). Some studies have shown that YAP1 promotes hepatic stellate cell activation and liver fibrosis, while inhibition of YAP1 blocks fibrogenesis in mice (Mannaerts et al., 2015; Du et al., 2018). Our previous research demonstrated that mice exposed to rare earth dust (Nd_2O_3)

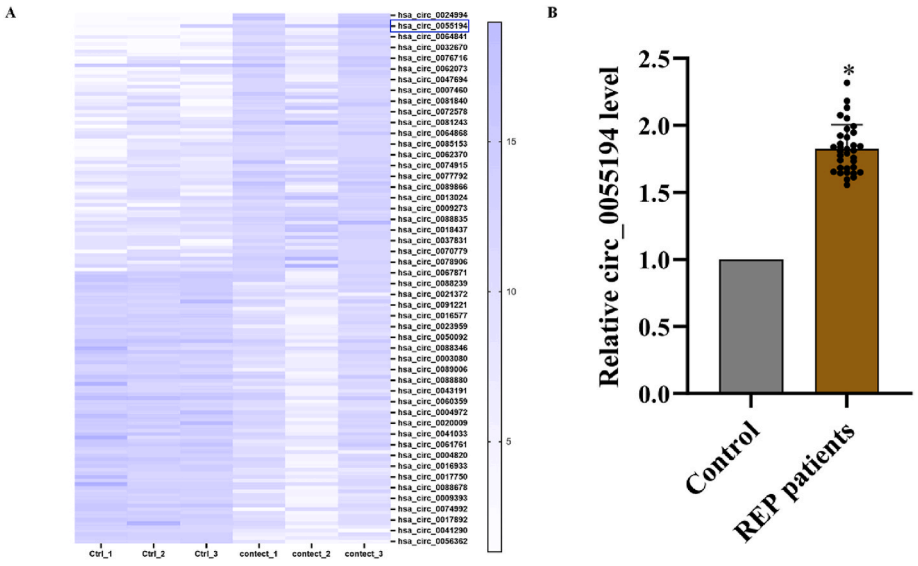

Fig. 1. For REP patients, the serum exosomes levels of circ_0055194 are elevated. High-throughput RNA sequencing was conducted on plasma samples obtained from patients diagnosed with rare earth pneumoconiosis. (A) A heatmap is presented, depicting the differential expression of circRNAs in the serum exosomes of three patients with REP. (B)The expression levels of circ_0055194 in the serum of REP patients were significantly elevated by qRT-PCR. Data are reported as mean ± SD, with n = 36. *P < 0.05, ddifferent from the control group of REP.

developed lung injury and fibrosis (Bu et al., 2022). Mice were exposed to Nd_2O_3 with different concentrations (0, 500, 1000, 2000 mg/m^3) for 2 h on one day, then harvested 7, 28 or 56 days later. HE staining and Masson staining showed that inflammatory cell infiltration could be seen in the alveolar cavity after 7 days of exposure, and the highest number of Nd_2O_3 group was 2000 mg/m^3. At 28 days, some blue collagen fibers were deposited in the lung interstitial, and some nodular structures of varying sizes appeared in the lung tissue of mice. There are some filament network of collagen fibers in the nodules, forming cellular nodules, accompanied by inflammatory cell infiltration and interstitial fibrosis. After 56 days of exposure, the number of nodules increased, some nodules fused, and interstitial fibrosis became more obvious with the increase of exposure dose. A blinded protocol was implemented for histopathological evaluation, and lung tissues from three randomly selected mice per experimental group were processed, with three serial sections generated per tissue. Five non-overlapping microscopic fields per section were imaged for systematic analysis. Fibrotic area percentage was quantified using Image J software with standardized thresholding algorithms, followed by statistical validation via GraphPad 6.0 (Fig. 2A and B). Furthermore, qRT-PCR analysis of lung tissue showed upregulated circ_0013556 levels and downregulated miR-665 levels in Nd_2O_3-induced lung tissue fibrosis of mice compared to controls (Fig. 2C and D). Western blot analysis demonstrated a time-dependent upregulation of YAP1, Twist, collagen I, and α-SMA protein expression in murine lung tissues following Nd_2O_3 exposure. The gray value of protein band were quantified using Image J software with normalization to GAPDH as controls, with triplicate biological replicates for each group (Fig. 2E and F). The results indicate that Nd_2O_3-induced lung tissue fibrosis in mice, as the exposure dose and duration increase, circ_0013556 expression increases, targeting and downregulating miR-665, activating the YAP1/Twist axis, and exacerbating pulmonary fibrosis.

3.3. *Knock-down of circ_0013556 increased miR-665 levels, blocked Yap1/Twist activation, and fibrosis was inhibited in Nd_2O_3-induced lung tissue of mice*

To investigate whether circ_0013556 plays a role in Nd_2O_3-induced pulmonary fibrosis of mice, we employed tracheal infusion to administer 0.1 mL of circ_0013556 gRNA(or sh-NC) AAV9 adenovirus suspension and 0.1 mL of DIO-spCAS9 gene AAV9 adenovirus suspension into the mouse trachea. This procedure established the AAV9-sh-circ_0013556 group and AAV9-sh-NC group, which was subsequently exposed to Nd_2O_3 one week later.Mice in the AAV9-sh-circ_0013556 group, AAV9-sh-NC group, and Nd_2O_3 group (6–8 weeks old) were sacrificed at 7d, 28d, and 56d post-exposure to Nd_2O_3. The morphological and pathological changes of lung were observed by HE staining, IHC staining and Masson staining, and analyzed by Image J. Compared with AAV9-sh-NC group, AAV9-sh-circ_0013556 group decreased the infiltration of lung tissue inflammation cells, and the inflammation was controlled. The deposition of collagen fibers and nodoid structures in lung interstitium decreased. α-SMA is a marker of fibroblast activation and myofibroblast transformation. Immuno-histochemical results of α-SMA in 56-day mouse lung tissue showed that Nd_2O_3 exposure promoted the activation of fibroblasts in the lung, and the activation was inhibited after the elimination of circ_0013556 (Fig. 3A–C). Further, qRT-PCR results showed that circ_0013556 levels were downregulated in the lungs of mice in the AAV9-sh-circ_0013556 group compared to the Nd_2O_3 group, alleviating the downregulation of miR-665 (Fig. 3D and E). Western blot analysis, quantified using Image J, revealed no significant differences in

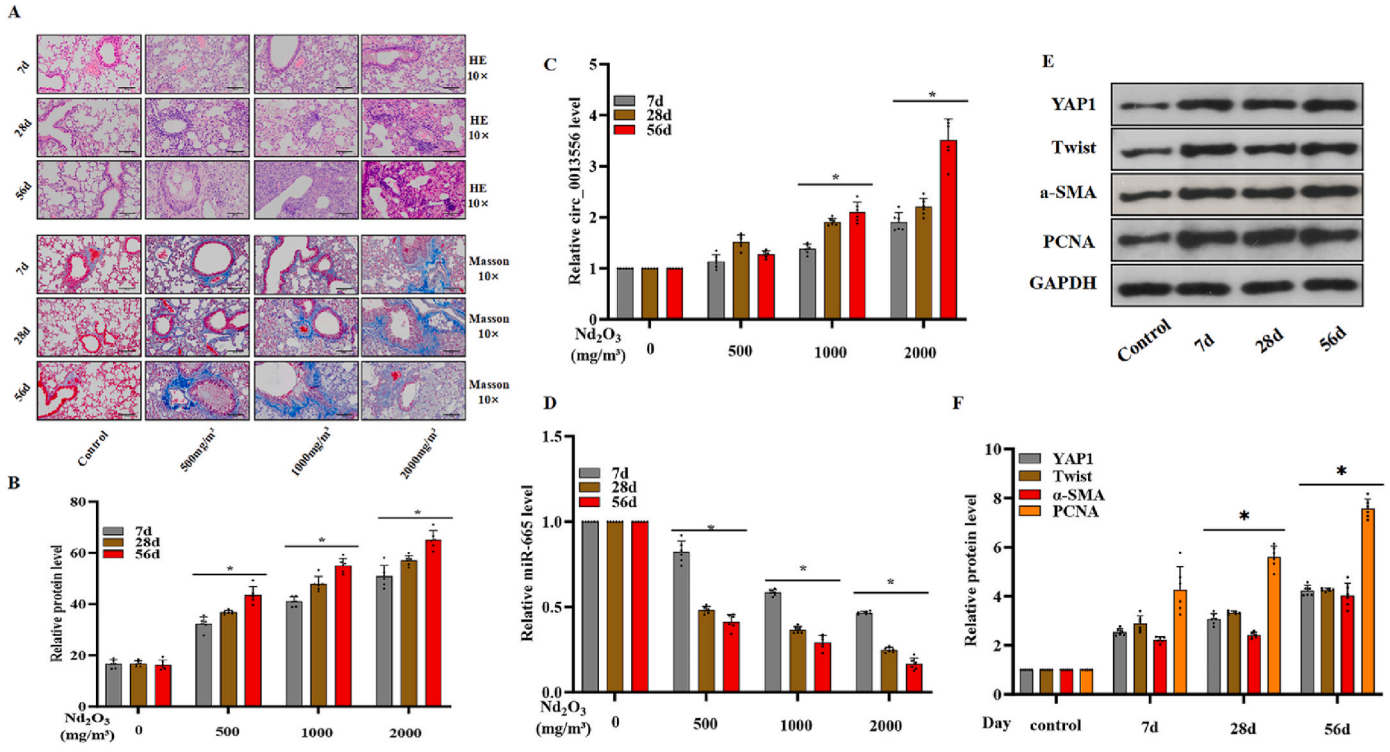

Fig. 2. In the murine model of Nd_2O_3-induced pulmonary fibrosis,circ_0013556 expression was increased, miR-665 level was decreased, and YAP1/Twist signaling pathway was activated. Mice exposed to rare earth Nd_2O_3 dust at concentrations of 500 mg/m^3, 1000 mg/m^3, and 2000 mg/m^{3}and subsequently euthanized under anesthesia after 7, 28, or 56 days. The band densities were quantitated using ImageJ software, with GAPDH levels measured in parallel as a control. (A) Representative micrographs depicting HE staining and Masson's trichrome staining in Nd_2O_3-induced lung fibrosiis of mice. (B) Collagen content in lung tissues was quantitated utilizing Image J software(means ± SD, n = 6). (C and D) The levels of circ_0013556 and miR-665 in lung tissues was assessed by qRT-PCR (means ± SD, n = 6). (E) Western blot analysis was conducted, and (F) the relative protein expression levels of YAP1, Twist, PCNA, and α-SMA in lung tissues were determined (means ± SD, n = 6). *P < 0.05, different from control mice.

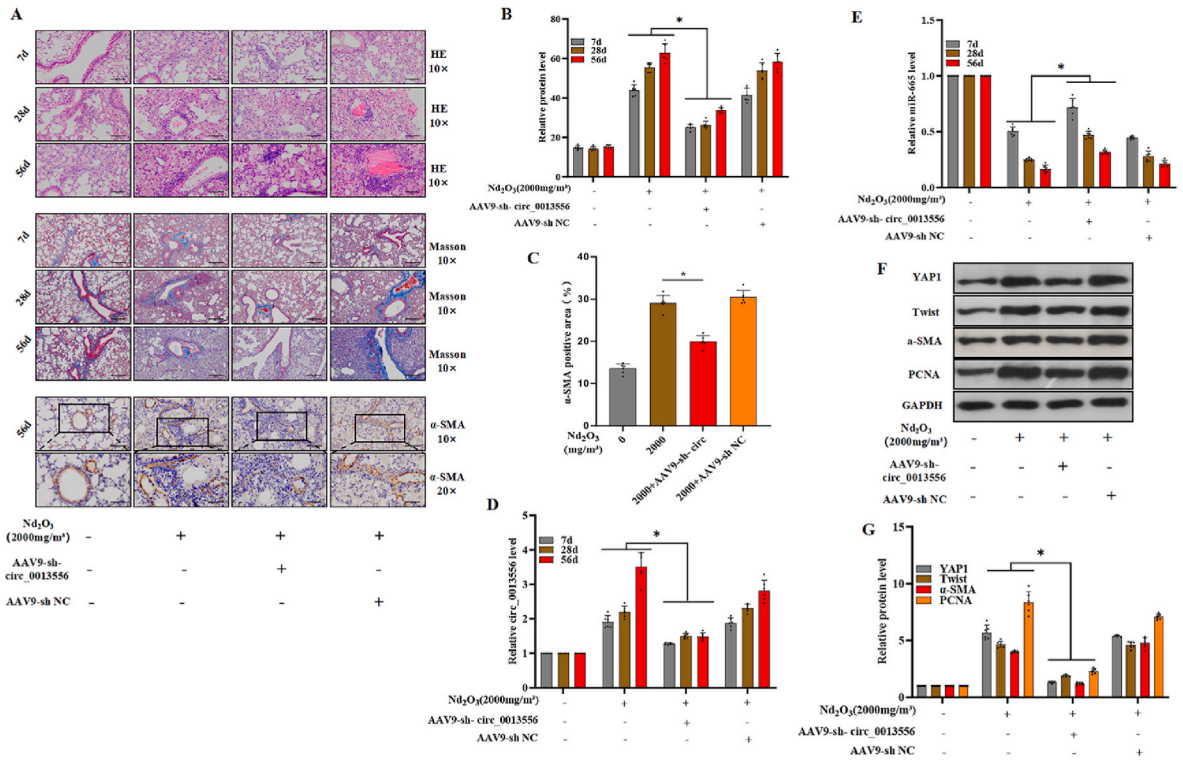

Fig. 3. Circ_0013556 knockdown prevents miR-665 decline, YAP1/Twist activation, and Nd_2O_3-induced lung fibrosis in mice. Circ_0013556 knockout (AAV9-sh-circ_0013556) mice and control (AAV9-sh-NC) mice aged 6–8 weeks were exposed to Nd_2O_3 dust at concentrations of 2000 mg/m^3. Image J software was used to quantitatively analyze the gray values of protein bands and GAPDH protein levels as control. (A) Representative micrographs of lung tissue stained with HE, Masson's trichrome, and immunohistochemistry (IHC) for α-SMA are presented. (B and C) Quantitative assessment of collagen and α-SMA content in mouse lung tissue was performed using ImageJ software(means ± SD, n = 6). (D and E) The levels of circ_0013556 and miR-665 in lung tissue were detected by qRT-PCR(means ± SD, n = 6). (F) Western blot analysis was carried out, and (G) the relative protein levels of YAP1, Twist, PCNA, and α-SMA in lung tissue were determined (means ± SD, n = 6). *P < 0.05, different from the AAV9-sh-circ_0013556 group.

α-SMA, collagen I, YAP1, and Twist levels between the AV9-sh-NC group and the Nd_2O_3 group when exposed to 2000 mg/m^3 Nd_2O_3, In contrast, the AAV9-sh-circ_0013556 group exhibited a significant reduction in these markers compared to both aforementioned groups (Fig. 3F and G). These findings indicate that the knockdown of circ_0013556 mitigates the downregulation of miR-665, alleviates YAP1/Twist axis activation and pulmonary fibrosis induced by Nd_2O_3 exposure in mice, indicating that circ_0013556 circ_0013556 plays a mediating role in Nd_2O_3-induced pulmonary fibrosis.

3.4. In a co-culture system, the treatment of THP-M cells with Nd_2O_3 increased the expression of circ_0055194, which subsequently acted on miR-665 of HELF cells via exosomes, thereby extensively activating the YAP1/Twist signaling pathway

We have confirmed elevated levels of circ_0055194 in the serum exosomes ncRNA expression profiles of REP patients, as well as increased circ_0013556 levels and fibrotic changes in the lungs of mice. Subsequently, we examined the scenario involving HELF cells cocultured with THP-M cells treated with Nd_2O_3. We hypothesized that circ_0055194 derived from exosomes (Exos) of Nd_2O_3-treated THP-M cells plays a role in facilitating the activation of the YAP1/Twist pathway via miR-665 in HELF cells. To test this hypothesis, THP-M cells were exposed to 0, 6.25, 12.5, or 25 μg/mL of Nd_2O_3 for 24 h before coculture with HELF cells. Subsequently, Nd_2O_3-treated THP-M cells, their exosomes (Nd_2O_3-THP-M-Exos), and the cocultured HELF cells were collected.

To confirm the circular structure of circ_0055194, total RNA extracted from THP-M cells was subjected to RNase R treatment prior to reverse transcription. Subsequently, the levels of circ_0055194 were quantified. The results demonstrated that the levels of circ_0055194 remained largely unchange (Fig. 4A). Next, through nuclear-cytoplasmic fractionation followed by qRT-PCR, it was observed that circ_0055194 is predominantly localized in the cytoplasmic (Fig. 4B). Furthermore, The binding of circ_0055194 and miR-665 was detected using RNA pull-down, and the qRT-PCR results showed that the enrichment and abundance ratio of the biotinylated miR-665 sense strand to the miR-665 antisense strand to circ_0055194 is much higher, providing strong evidence for the interaction between miR-665 and circ_0055194 (Fig. 4C). The luciferase assay report showed that compared with the NC group, miR-665 significantly down-regulated the luciferase activity in YAP1-3UTR-WT group, indicating that miR-665 had a direct binding effect with YAP1. After binding site mutation, miR-665 could not down-regulate luciferase expression in YAP1-3 UTR-MUT group compared with NC group, indicating that the mutation was successful (Fig. 4D). Based on previous research, we evaluated the effects of Nd_2O_3 exposure on lung cell-cell communication and established a co-culture cell model to identify factors associated with impaired crosstalk between THP-M cells and HELF cells (Fig. 4E). Fibroblast activation, marked by elevated expression of α-SMA and increased extracellular matrix (ECM) deposition, plays a critical role in the progression of pulmonary fibrosis (Heinzelmannet al., 2018).

Exosomes are widely involved in intercellular communication contributing to the maintenance lung tissue homeostasis and normal function (Meldolesi, 2018; Kalluri and LeBleu, 2020). After exposing THP-M cells to Nd_2O_3 for 24 h (referred to as Nd_2O_3-THP-M cells), Exosomes with a diameter ≤200 nm were isolated. Exosomes derived from Nd_2O_3-treated THP-M cells and those from untreated THP-M cells were quantitated and characterized employing transmission electron microscopy and dynamic light scattering. The results indicated no

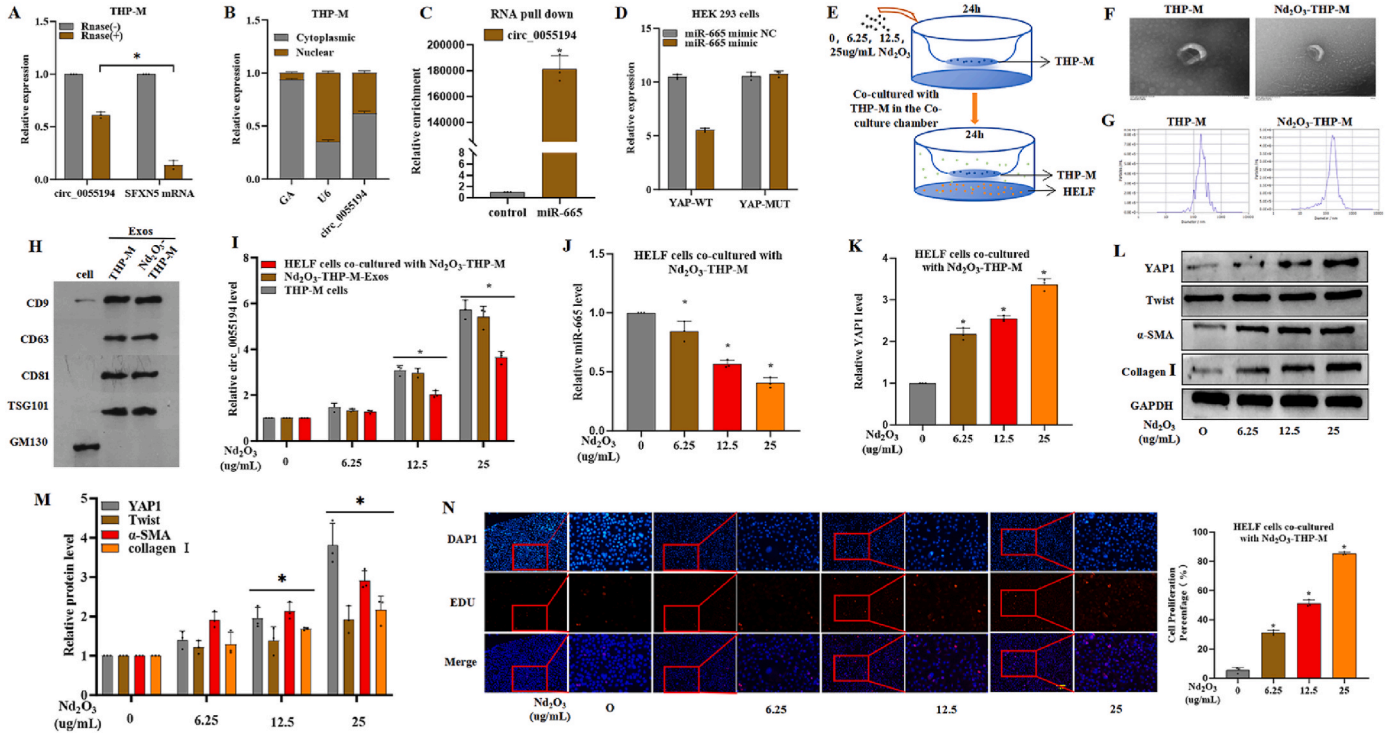

Fig. 4. Nd_2O_3-THP-M exosomes elevated circ_0055194 in HELF, reduced miR-655, and activated YAP1/Twist. THP-M-Exos are exosomal vesicles derived from THP-1 cells that have been induced to differentiate into THP-M macrophages and subsequently release exosomes. Nd_2O_3-THP-M-Exos, originate from THP-M cells that have been treated with Nd_2O_3 at concentrations of (0, 6.25, 12.5, and 25 μg/mL), and HELF cells were cultivated alongside THP-M cells that had been pretreated with 0, 6.25, 12.5, and25 μg/mL Nd_2O_3 for 24 h. Band densities were quantitated using ImageJ software, with GAPDH levels assessed in parallel as a control. For coculture experiments, (A) RNase R (2.5 U/μg, 37 °C, 15 min) treatment was applied to cell extracts to eliminate linear transcripts, leaving circRNA intact. The resistance of the RNA to RNase R degradation was subsequently assessed by qRT-PCR (means ± SD, n = 3).(B) Cytoplasmic and nuclear fractionation was carried out to detect the presence of circ_0055194(means ± SD, n = 3).(C) A miR-665 pull-down assay followed by qPCR was performed(means ± SD, n = 3). (D) Luciferase reporter gene experiments were conducted using HEK 293 cells(means ± SD, n = 3). (E) Co-culture of THP-M cells and HELF cells.(F) Transmission electron microscopy (TEM) images of exosomes are presented (scale bar = 200 nm).(G) The particle number and size distribution of THP-M-Exos and Nd_2O_3-THP-M-Exos were determined using dynamic light scattering with a ZetaView nanoparticle tracker (ParticleMetrix, Germany).(H) Western blot analysis was performed to detect the presence of CD9, CD63, CD81, TSG101, and GM130 (a Golgi marker protein) in both exosomes and cells. (I) Further, qRT-PCR was utilized to quantify circ_0055194 levels in THP-M cells, exosomes, and HELF cells(means ± SD, n = 3). (J and K) The miR-665 and YAP1 mRNA levels in HELF cells were measured by qRT-PCR (means ± SD, n = 3). (L) Western blot analysis was conducted, and (M) the relative protein levels of YAP1, Twist, Collagen I, and α-SMA in HELF cells were determined (means ± SD, n = 3). (N) EDU/DAPI ratio showed that the increased circ_0055194 level promoted the proliferation of HELF cells(means ± SD, n = 3). *P < 0.05, different from empty vector group or HELF cells co-cultured with normal THP-M cells.

statistically significant differences in either particle size or number between the two exosome populations (Fig. 4F and G). Furthermore, a Western blot analysis was performed to evaluate the expression levels of the exosomal markers CD9, CD63, CD81, and TSG101, as well as the negative control marker GM130 (golgi apparatus marker) (Fig. 4H).

Following a 24-h coculture of HELF cells with Nd_2O_3-THP-M cells, qRT-PCR analysis revealed that, compared to the control group, there were concurrent elevations in circ_0055194 expression levels in Nd_2O_3-THP-M cells, Nd_2O_3-THP-M-derived exosomes. Additionally, there were corresponding reductions and augmentations in miR-665 and YAP1 mRNA levels, respectively, within the HELF cells (Fig. 4I–K).

With increasing Nd_2O_3 exposure concentrations, Western blot results analyzed using ImageJ showed increased levels of YAP1, Twist, α-SMA, and collagen I (Fig. 4L and M). The EDU cell proliferation kit was employed to assess the proliferative capacity of HELF cells following coculture. In the assay, blue represents DAPI staining (nuclear marker), red represents EDU incorporation (proliferation marker), and the EDU/DAPI ratio serves as an indicator of the relative proliferative ability (Fig. 4N). In summary, Nd_2O_3-THP-M cells may induce increased circ_0055194 levels, and decreased miR-665 levels in HELF cells through exosomal transfer, thereby activating the YAP1/Twist axis and facilitating HELF cell proliferation, differentiation into myofibroblasts, and ECM deposition.

3.5. After knocking down circ_0055194 and coculture, the upregulation of circ_0055194 in HELF cells affected by Nd_2O_3-THP-M-Exos was alleviated, miR-665 levels rebounded, and the YAP1/Twist signaling pathway was inhibited

To further verify whether Nd_2O_3-THP-M cells may induce the increase of circ_0055194 level and the decrease of miR-665 level in HELF cells through exosomes to activate the YAP1/Twist axis and promot HELF cell proliferation. we transfected THP-M cells with circ_0055194 siRNA or siRNA-NC and then exposed them to 25 μg/mL of Nd_2O_3 for 24 h before coculture with HELF cells (Fig. 5A). By knocking down circ_0055194, the levels of circ_0055194 in Nd_2O_3-THP-M cells and Nd_2O_3-THP-M-Exos decreased, leading to a synchronous downregulation of circ_0055194 levels in cocultured HELF cells (Fig. 5B). The downregulation of circ_0055194 resulted in increased miR-665 levels and downregulated YAP1 mRNA in HELF cells (Fig. 5C and D), as well as decreased protein levels of YAP1, Twist, α-SMA, and collagen I (Fig. 5E and F) and inhibited fibroblast proliferation (Fig. 5G).

Overall, after knocking down circ_0055194, Nd_2O_3-THP-M cells acted on cocultured HELF cells via exosomes, inhibiting the YAP1/Twist axis and proliferation, and alleviating differentiation into myofibroblasts and ECM deposition.

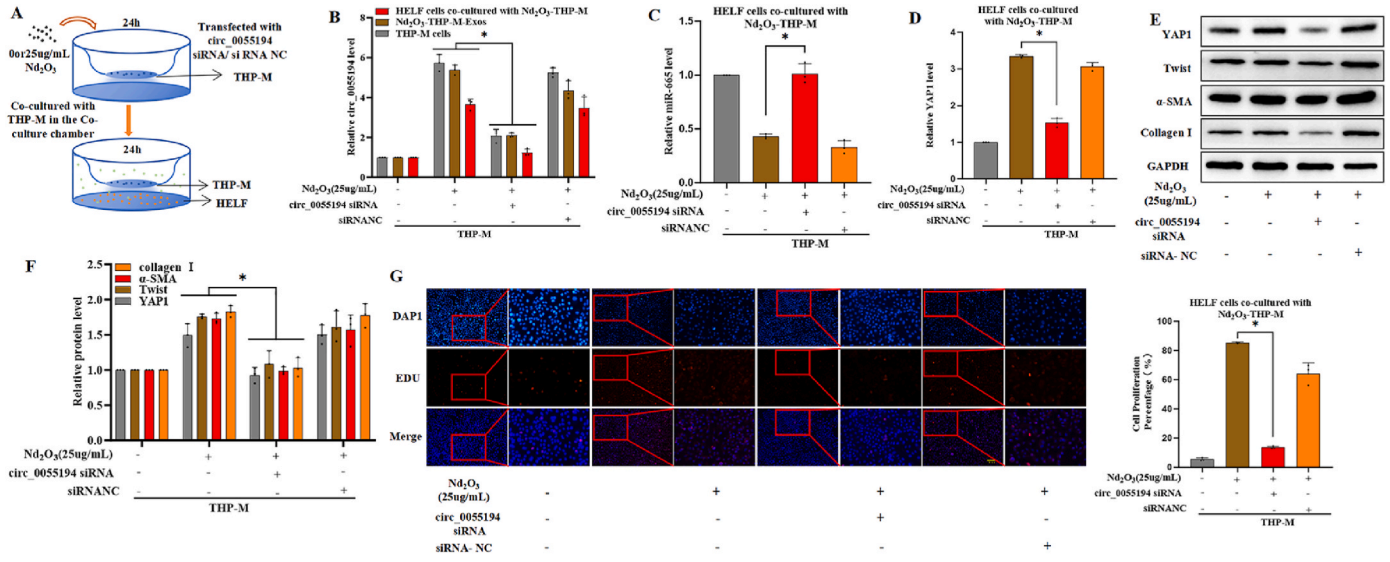

Fig. 5. Exosomal circ_0055194 from Nd_2O_3-THP-M cells promotes YAP/Twist axis, proliferation, myofibroblast differentiation, and ECM accumulation in HELF cells. THP-M cells were transfected with either circ_0055194-specific siRNA or a non-targeting siRNA control (siRNA NC). Subsequently, these cells were exposed to Nd_2O_3 at a concentration of 0 or 25 μg/mL for 24 h. Band densities were then quantified using ImageJ software, with GAPDH serving as a loading control to normalize the data. (A) Co-culture of THP-M cells and HELF cells. (B) The levels of circ_0055194 were assessed using qRT-PCR in THP-M cell, Nd_2O_3-THP-M-Exos and HELF cells (means ± SD, n = 3). (C) and (D) Additionally, qRT-PCR was employed to measure the levels of miR-665 and YAP1 mRNA in HELF cells (means ± SD, n = 3). (E) Western blot analysis was performed to examine protein expression, and (F) the relative levels of YAP1, Twist, Collagen I, and α-SMA in HELF cells were quantified (means ± SD, n = 3). (G) The EDU/DAPI ratio showed that HELF cell proliferation was inhibited after circ_0055194 knockdown (means ± SD, n = 3). *P < 0.05 different from HELF cells co-cultured with siRNA NC -THP-M cells.

3.6. Overexpression of miR-665 in HELF cells followed by coculture resulted in miR-665 levels that were unaffected by circ_0055194 in Exos, and the YAP1/Twist signaling pathway was inhibited

To determine whether the upregulated circ_0055194 in HELF cells after coculture with Nd_2O_3-THP-M cells competitively inhibits miR-665 levels through sponge adsorption, we cocultured Nd_2O_3-THP-M cells with HELF cells transfected with miR-665 mimic or miRNA NC (Fig. 6A). The effect of circ_0055194 in Exos was blocked by overexpressed miR-665, and YAP1 mRNA levels were downregulated (Fig. 6B and C). The levels of YAP1, Twist, collagen I, and α-SMA were alleviated (Fig. 6D and E), and the proliferation level of HELF cells was inhibited (Fig. 6F). The

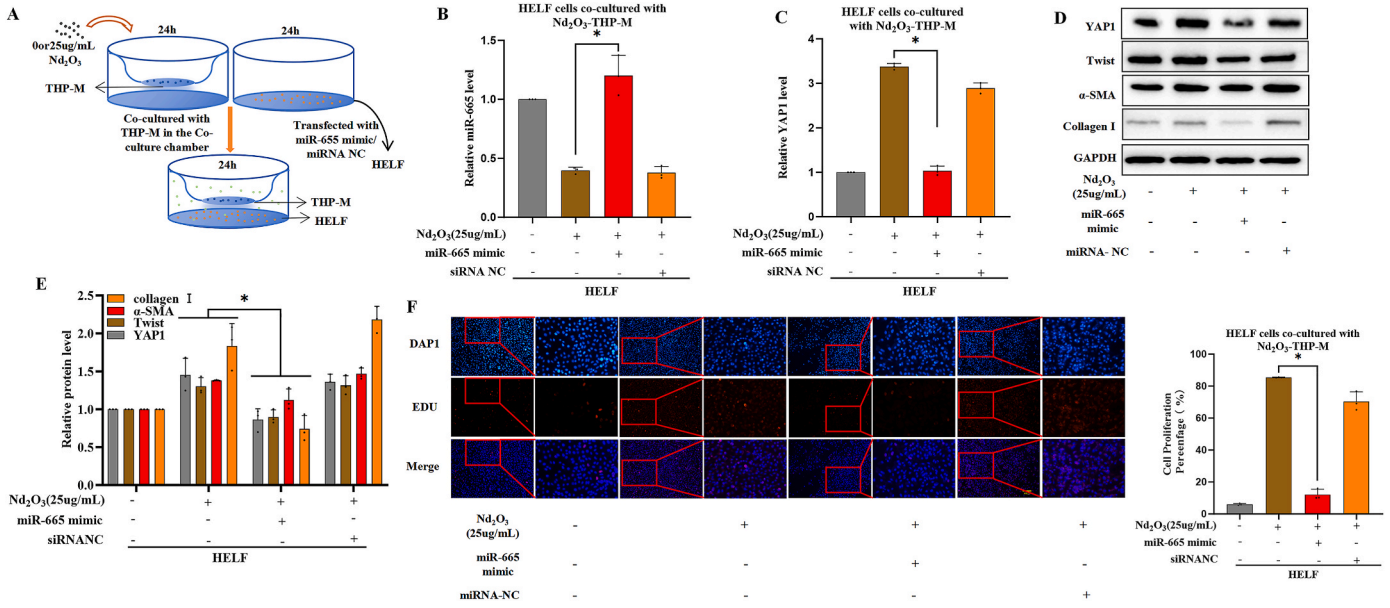

Fig. 6. Exosomal circ_0055194 from Nd_2O_3-THP-M cells activates YAP/Twist, proliferation, and differentiation in HELF via targeting miR-665. THP-M cells, were treated with Nd_2O_3 at concentrations of 0 or 25 μg/mL for 24 h. Subsequently, these cells were cocultured with HELF cells that had been transfected with either a miR-665 mimic or a non-targeting miRNA control (miRNA NC) for an additional 24 h. Band densities were then quantified using ImageJ software, with GAPDH serving as a loading control for normalization.(A) Co-culture of THP-M cells and HELF cells. (B and C) The miR-665 and YAP1 mRNA levels in HELF cells were measured by qRT-PCR (means ± SD, n = 3). (D) Western blot analysis was performed to assess protein expression, and (E) the relative levels of YAP1, Twist, Collagen I, and α-SMA in HELF cells were quantified (mean ± SD, n = 3). (F) The EDU/DAPI ratio showed that HELF cell proliferation was inhibited after overexpression of miR-665 (mean ± SD, n = 3). *P < 0.05 different from miRNA-NC HELF cells co-cultured with THP-M cells.

results showed that that overexpression of miR-665 alleviated the activation of the YAP1/Twist axis, cell proliferation, and ECM deposition caused by elevated circ_0055194 levels.

3.7. In HELF cells, circ_0055194 from Exos of Nd_2O_3-treated THP-M cells is involved in cell proliferation and ECM deposition through the miR-665/YAP1/Twist signaling pathway

We cocultured Nd_2O_3-THP-M cells transfected with siRNA-NC or circ_0055194 siRNA with HELF cells transfected with miRNA NC or miR-665 inhibitor (Fig. 7A). The reduction in YAP1 mRNA levels caused by circ_0055194 siRNA was restored by the miR-665 inhibitor (Fig. 7B and C). The downregulation of circ_0055194 in Exos from Nd_2O_3-THP-M cells blocked changes in collagen I, YAP1, Twist, and α-SMA proteins, but the inhibition of miR-665 reversed the effect of circ_0055194 siRNA (Fig. 7D and E). The EDU results showed that the inhibition of HELF cell proliferation caused by reduced circ_0055194 expression was reversed by the knockdown of miR-665 (Fig. 7F). Inhibition of miR-665 in HELF cells restored the activation of the YAP1/Twist axis, as well as promoted ECM deposition and myofibroblast transformation blocked by circ_0055194 siRNA. In conclusion, we have demonstrated that the upregulation of circ_0055194 in THP-M cells exposed to Nd_2O_3 influences cocultured HELF cells through exosomal transfer. Specifically, circ_0055194 functions as a sponge molecule to downregulate miR-665 levels, thereby activating the YAP1/Twist signaling axis. This activation promotes fibroblast proliferation, differentiation into myofibroblasts, and extracellular matrix (ECM) deposition (see Fig. 8).

4. Discussion

Epigenetic modifications exert a crucial influence on the development of lung inflammation and profibrotic responses in pneumoconiosis, and lncRNAs, circRNAs, and miRNAs have emerged as potential therapeutic targets for the treatment of lung diseases (Li et al., 2022; Liu et al., 2022). Knockdown of circ_PWWP2A has been shown to inhibit TGF-β-induced lung fibroblast activation and alleviate bleomycin-induced lung fibrosis in rats through the miR-27b-3p/GATA3 axis (Su et al., 2023). Our previous studies demonstrated that exposure to Nd_2O_3 in mice or rats led to the sponging of miR-29a-3p by LncRNA H19 in lung tissue, inducing inflammatory cell infiltration and NF-κB pathway activation, ultimately resulting in lung fibrosis (Wang et al., 2016; Bu et al., 2022). However, the role and molecular mechanisms of circRNAs in Nd_2O_3-induced lung fibrosis remain to be investigated.

Early diagnosis of lung fibrosis is particularly challenging due to confounding factors, and research on therapeutic targets is scarce (Wang et al., 2016; Bu et al., 2022). Given the stability of circRNAs, our research offers an additional option for early diagnosis and selection of therapeutic targets for lung fibrosis. In the present studies, we first profiled ncRNA expression in the serum of REP patients and identified elevated expression of circ_0055194.Moreove, the expression levels of circ_0055194 in the blood of REP patients were significantly elevated by qRT-PCR. Additionally, we found that levels of circ_0013556 was significantly increased in the lung of mice exposed to Nd_2O_3, and the levels of α-SMA and PCNA,as fibrotic factor, were also elevated. Furthermore, after intranasal and oral exposure to Nd_2O_3, mice in the AAV9-sh-circ_0013556 group exhibited reduced levels of circ_0013556, leading to decreased α-SMA and PCNA expression, and ultimately

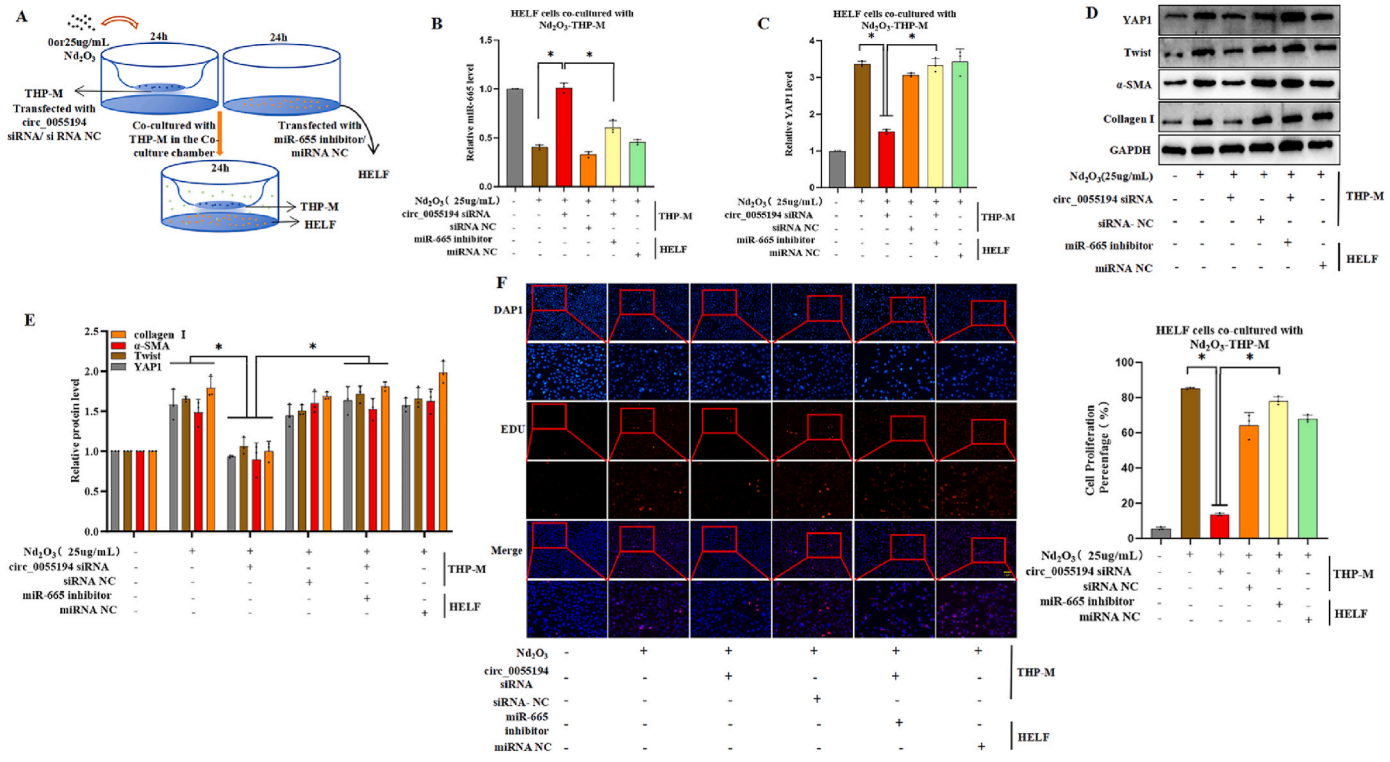

Fig. 7. Exosomal circ_0055194 from Nd_2O_3-THP-M cells in HELF cells promotes proliferation, differentiation, and ECM via miR-665/YAP1/Twist axis. THP-M cells, were transfected with either circ_0055194 siRNA or a non-targeting siRNA control (siRNA NC). These cells were then exposed to Nd_2O_3 at concentrations of 0 or 25 μg/mL for 24 h. Subsequently, they were cocultured with HELF cells that had been transfected with a miR-665 inhibitor or a non-targeting miRNA control (miRNA NC) for an additional 24 h. Band densities were quantified using ImageJ software, with GAPDH serving as a loading control for normalization.(A) Co-culture of THP-M cells and HELF cells. (B and C) The miR-665 and YAP1 mRNA levels in HELF cells were measured by qRT-PCR (means ± SD, n = 3). (D) Western blot analysis was performed to examine protein expression, and (E) the relative levels of YAP1, Twist, Collagen I, and α-SMA in HELF cells were quantified (means ± SD, n = 3). (F) The EDU/DAPI ratio demonstrated that the knockdown of miR-665 significantly reversed the inhibitory effect on HELF cell proliferation induced by the depletion of circ_0055194 (means ± SD, n = 3). *P < 0.05 different from HELF cells co-cultured with circ_0055194 siRNA THP-M cells.

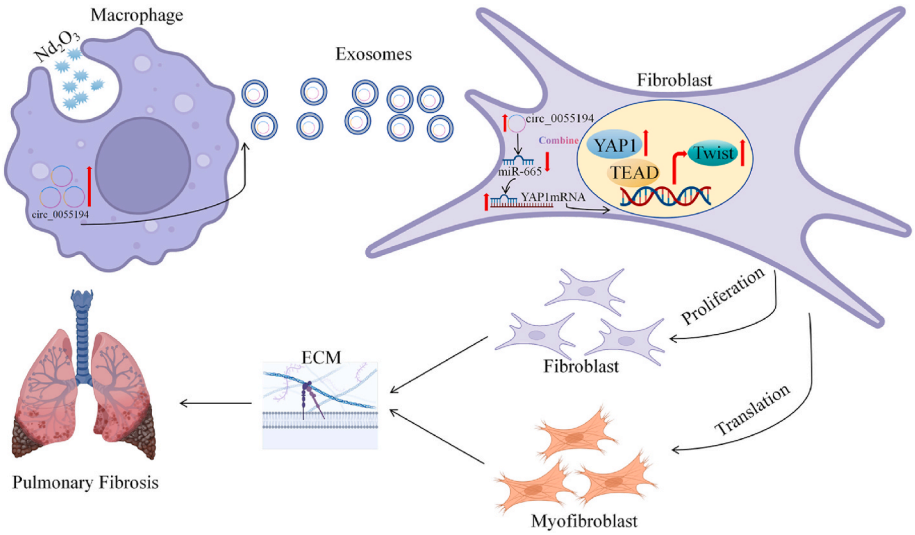

Fig. 8. Macrophages-derived exosomal circ_0055194 regulating miR-665/YAP1/Twist axis is involved in pulmonary fibrosis induced by Nd_2O_3.

alleviated lung fibrosis compared to mice in the Nd_2O_3 group.

Macrophages are the first line of defense against exogenous substances and recruit inflammatory cells and fibroblasts upon damage. Macrophages secrete exosomes, leading to fibroblast activation and differentiation into myofibroblasts and ECM deposition (Kishore and Petrek, 2021; Pokhrealet al., 2023). Studies have found that circ_0020256 in macrophage-secreted exosomes promotes the proliferation, migration, and invasion of cholangiocarcinoma cells, regulated through the circ_00200256/miR-432-5p/E2F3 axis (Chen et al., 2022). Therefore, in the present study, We extracted and characterized exosomes from THP-M cells either exposed to or not exposed to Nd_2O_3, and detected the levels of circ_0055194 in the exosomes, which were positively correlated with the exposure dose. Specifically, the circ_0055194 levels in exosomes from THP-M cell exposed to Nd_2O_3 were significantly increased. And then we cocultured THP-M cells exposed to Nd_2O_3 with HELF cells to explore the impact of intercellular communication and mediator transmission on myofibroblast differentiation and ECM deposition. Interestingly, we found elevated circ_0055194 levels in HELF cells. After knocking down the circ-0055194 of macrophage, the circ_0055194 of exosomes was decreased after exposure to Nd_2O_3, and the level of circ_0055194 in fibroblasts co-cultured with macrophages was also decreased. In conclusion, macrophages-derived exosomal circ_0055194 may play a role in REP.

CircRNAs possess the ability to modulate the levels of miRNAs and subsequently impacting the fibrotic process (Liu et al., 2023). Studies have found that overexpression of circZNF609 can attenuate SO_2-induced lung fibrosis in mice and inhibit TGF-β1-induced fibroblast activation, regulating lung fibrosis through the miR-145-5p/KLF4 axis (Liu et al., 2022). Circ_0007535 acts as a sponge for miR-18a-5p, modulating the expression of its downstream target TGFBR1, and consequently facilitating TGF-β1-induced lung fibrosis. Knockdown of circ_0007535 alleviated TGF-β1-induced proliferation, differentiation, inflammatory responses, and ECM deposition in human embryonic lung fibroblasts (HFL1), while inhibition of miR-18a-5p reversed all the effects of circ_00007535 reduction of expression in TGF-β1-treated HFL1 cells (Shenet al., 2023). In our prior research, we identified the abnormal expression of circ_0055194 through transcriptome sequencing of serum exosomes in REP patients, and this finding was subsequently validated in a larger cohort of serum exosome samples from REP patients. Prediction by bioinformatics,we found that hsa_circ_0055194 (and mmu_circ_0013556) can serve as ceRNAs for miR-665. Moreover, further detection showed that the miR-665 level was significantly reduced in HELF cells cocultured with Nd_2O_3-THP-M cells and in lung tissue of mice exposed to Nd_2O_3. Subsequently, we validated the adsorption of circ_0055194 to miR-665 using a pull-down assay. Both in vitro and in vivo results demonstrated downregulation of hsa_circ_0055194 (and mmu_circ_0013556) in HELF cells cocultured with Nd_2O_3-THP-M cells and in lung tissue of mice exposed to Nd_2O_3, accompanied by reversion of miR-665 levels, and inhibited proliferation and differentiation of fibroblast and Pulmonary fibrosis. These results suggested that the circ_0013556 binding miR-665 is involved in Nd_2O_3 induced pulmonary fibrosis.

The proliferation and differentiation of fibroblast is a key node of pulmonary fibrosis, and YAP1,as a key cofactor activating the transcription factor of Twist, regulates of cell proliferation and transformation (Zhanget al., 2023). Deposited ECM proteins (such as Collagen I and α-SMA) produced by myofibroblasts ultimately lead to PF, while downregulation of YAP1 inhibits ECM deposition and improves lung fibrosis both in vitro and in vivo (Chen et al., 2019). Our experimental results showed increased levels of α-SMA and PCNA, markers of fibroblast proliferation and differentiation, as well as YAP1, and Twist were increased, and pulmonary fibrosis was significantly enhanced in mice exposed to Nd_2O_3. With the knockdown of circ_0013556, the expression leveles of α-SMA, PCNA, YAP1 and Twist were inhibited, resulting in alleviating pulmonary fibrosis. These results suggested that circ_0013556 played an important role in Nd_2O_3 induced pulmonary fibrosis, and circ_0013556 may regulate the expression of YAP1 by adsorbing miR-665 and subsequently up-regulate the expression of Twist, thereby inducing the proliferation and differentiation of fibroblasts and ultimately causing pulmonary fibrosis. Next, in the present study, it was certificated that the binding of miR-665 to 3′UTR of YAP1mRNA was verified through luciferase reporter gene experiments. Overexpression of miR-665 in HELF cells cocultured with Nd_2O_3-THP-M cells targeting YAP1 reduced Twist expression and reversed fibroblast activation and pulmonary fibrosis. Knockdown of circ_0055194 of macrophages while the downregulation of miR-665 of HELF cells, YAP1, Twist, Collagen I and α-SMA were increased, and the proliferation of fibroblast was significantly enhanced that highlighted the role of exosomal circ_0013556 from macrophages regulating miR-665/YAP1/Twist axis in Nd_2O_3 inducing pulmonary fibrosis. In conclusion, our study demonstrates that the circ_0055194 regulates the YAP1/Twist axis inducing the proliferation and differentiation of fibroblasts and EMC secretion through miR-665, influencing lung fibrosis via exosome-mediated macrophage-fibroblast communication. We identified a significant upregulation of circ_0055194 in serum exosomes from REP patients, which was subsequently validated in both in vivo and in vitro experimental systems. It is important to highlight that our co-culture system cannot entirely exclude the potential contribution of

other soluble cytokines or enzymes, in addition to exosomes, to the pro-fibrotic effect. Nevertheless, our findings demonstrate that exosomal circ_0055194 plays a critical role in promoting fibrosis, as evidenced by knockdown and rescue experiments. Specifically, we show that circ_0055194 mediates pulmonary fibrosis through the miR-665/YAP/Twist signaling axis. All in all, we cautiously propose that circ_0055194 may serve as a potential biomarker or therapeutic target for REP and, more broadly, pulmonary fibrotic diseases. Furthermore, the experiments we conducted were accomplished using human embryonic lung fibroblasts (HELF) instead of adult lung fibroblasts. In the future, we will delve deeper into the role of adult lung fibroblasts in the process of fibrosis.

5. Conclusion

This study reveals that in human embryonic lung fibroblast (HELF) cells and C57BL/6J mice, Nd_2O_3 modulates the YAP1/Twist axis via exosomes released by injured macrophages, ultimately resulting in extracellular matrix (ECM) deposition and lung fibrosis. This regulatory effect is mediated by circ_0055194, which functions as a miR-665 sponge, thereby negatively regulating miR-665 and leading to the overexpression of YAP1/Twist, which in turn enhances ECM secretion. Our findings indicate that exosomal circ_0055194 holds promise as an early biomarker for the prevention and management of lung injury and fibrosis induced by rare earth elements.

CRediT authorship contribution statement

Yuanqi He: Writing – review & editing, Writing – original draft, Visualization, Validation, Software, Methodology, Investigation, Formal analysis, Data curation, Conceptualization. **Yuhang Zhao:** Software, Resources, Investigation, Formal analysis, Conceptualization. **Kai Wu:** Visualization, Validation, Supervision, Formal analysis, Data curation. **Danyan Qi:** Validation, Formal analysis, Data curation. **Yupeng Ma:** Supervision, Software, Formal analysis, Data curation. **Wenjie Li:** Supervision, Investigation, Data curation, Conceptualization. **Xiangyu Chang:** Supervision, Investigation, Funding acquisition, Data curation, Conceptualization. **Suhua Wang:** Writing – review & editing, Resources, Funding acquisition, Data curation, Conceptualization. **Yanrong Gao:** Writing – review & editing, Validation, Supervision, Resources, Project administration, Funding acquisition, Formal analysis, Data curation, Conceptualization.

Ethics declarations

All animal procedures were reviewed and approved by the Animal Ethics Review Committee at Baotou Medical College.

Consent for publication

Not applicable.

Availability of data and materials

All data and materials presented in the current study along with additional files are available from the corresponding author on reasonable request.

Code availability

Not applicable.

Funding

This study were supported by the National Natural Science Foundation of China (grant number: 82241092 to W. S.)and the Inner Mongolia Natural Science Foundation (grant number: 2024MS08003 to G. Y.).

Declaration of competing interest

The authors declare that they have no known competing financial interests or personal relationships that could have appeared to influence the work reported in this paper.

Data availability

Data will be made available on request.

References

Bu, N., Gao, Y., Zhao, Y., Xia, H., Shi, X., Deng, Y., Wang, S., Li, Y., Lv, J., Liu, Q., Wang, S., 2022. LncRNA H19 via miR-29a-3p is involved in lung inflammation and pulmonary fibrosis induced by neodymium oxide. Ecotoxicol. Environ. Saf. 247, 114173.

Bu, N., Wang, S., Ma, Y., Xia, H., Zhao, Y., Shi, X., Liu, Q., Wang, S., Gao, Y., 2023. The lncRNA H19/miR-29a-3p/SNIP1/c-myc regulatory axis is involved in pulmonary fibrosis induced by Nd2O3. Toxicol. Sci. 197, 27–37.

Chen, X., Cheng, Y., Xiao, H., Feng, G., Deng, Y., Feng, Z., Chen, L., Han, X., Yang, Y., Dong, Z., Zhen, R., 2003. A 20-year follow-up study on the effects of long-term exposure to thorium dust. Chin Med J (Engl) 116, 692–694.

Chen, Y., Zhao, X., Sun, J., Su, W., Zhang, L., Li, Y., Liu, Y., Zhang, L., Lu, Y., Shan, H., Liang, H., 2019. YAP1/Twist promotes fibroblast activation and lung fibrosis that conferred by miR-15a loss in IPF. Cell Death Differ. 26, 1832–1844.

Chen, S., Chen, Z., Li, Z., Li, S., Wen, Z., Cao, L., Chen, Y., Xue, P., Li, H., Zhang, D., 2022. Tumor-associated macrophages promote cholangiocarcinoma progression via exosomal Circ_0020256. Cell Death Dis. 13, 94.

Conigliaro, A., Cicchini, C., 2018. Exosome-Mediated signaling in epithelial to mesenchymal transition and tumor progression. J. Clin. Med. 8.

Du, K., Hyun, J., Premont, R.T., Choi, S.S., Michelotti, G.A., Swiderska-Syn, M., Dalton, G.D., Thelen, E., Rizi, B.S., Jung, Y., Diehl, A.M., 2018. Hedgehog-YAP signaling pathway regulates glutaminolysis to control activation of hepatic stellate cells. Gastroenterology (New York, N. Y., 1943) 154, 1465–1479.

Gao, Y., Wang, S., He, Y., Ma, Y., Wang, S., 2025. Transcriptional profiling of exosomes derived from serum of patients with rare earth pneumoconiosis by RNA-sequencing and PI3K/Akt pathway is activated in lung of mice exposed to rare earth Nd(2)O(3). Toxicol. Lett. 404, 9–19.

Gwenzi, W., Mangori, L., Danha, C., Chaukura, N., Dunjana, N., Sanganyado, E., 2018. Sources, behaviour, and environmental and human health risks of high-technology rare earth elements as emerging contaminants. Sci. Total Environ. 636, 299–313.

Heinzelmann, K., Lehmann, M., Gerckens, M., Noskovičová, N., Frankenberger, M., Lindner, M., Hatz, R., Behr, J., Hilgendorff, A., Königshoff, M., Eickelberg, O., 2018. Cell-surface phenotyping identifies CD36 and CD97 as novel markers of fibroblast quiescence in lung fibrosis. Am. J. Physiol. Lung Cell. Mol. Physiol. 315, L682–L696.

Jeck, W.R., Sharpless, N.E., 2014. Detecting and characterizing circular RNAs. Nat. Biotechnol. 32, 453–461.

Kalluri, R., LeBleu, V.S., 2020. The biology, function, and biomedical applications of exosomes. SCIENCE 367.

Kishore, A., Petrek, M., 2021. Roles of macrophage polarization and macrophage-derived miRNAs in pulmonary fibrosis. Front. Immunol. 12, 678457.

Li, Y., Cheng, Z., Fan, H., Hao, C., Yao, W., 2022. Epigenetic changes and functions in pneumoconiosis. Oxid. Med. Cell. Longev. 2022, 2523066.

Lian, Z., Han, Y., Zhao, X., Xue, Y., Gu, X., 2022. Rare earth elements in the upland soils of northern China: spatial variation, relationships, and risk assessment. Chemosphere 307, 136062.

Liu, Y., Tang, G., Li, J., 2022. Long non-coding RNA NEAT1 participates in ventilator-induced lung injury by regulating miR-20b expression. Mol. Med. Rep. 25.

Liu, X., Wu, M., He, Y., Gui, C., Wen, W., Jiang, Z., Zhong, G., 2023. Construction and integrated analysis of the ceRNA network hsa_circ_0000672/miR-516a-5p/TRAF6 and its potential function in atrial fibrillation. Sci. Rep. 13, 7701.

Mannaerts, I., Leite, S.B., Verhulst, S., Claerhout, S., Eysackers, N., Thoen, L.F.R., Hoorens, A., Reynaert, H., Halder, G., van Grunsven, L.A., 2015. The Hippo pathway effector YAP controls mouse hepatic stellate cell activation. JOURNAL OF HEPATOLOGY 63, 679–688.

Meldolesi, J., 2018. Exosomes and ectosomes in intercellular communication. Curr. Biol. 28, R435–R444.

Pokhreal, D., Crestani, B., Helou, D.G., 2023. Macrophage implication in IPF: updates on immune, epigenetic, and metabolic pathways. Cells 12.

Shen, M., Wang, X., Chang, X., Li, Z., Jiang, N., Han, Z., Liu, X., 2023. Circ_0007535 upregulates TGFBR1 to promote pulmonary fibrosis in TGF-β1-treated lung fibroblasts via sequestering miR-18a-5p. Autoimmunity 56, 2259128.

Shi, X., Bai, Y., Gao, Y., Bu, N., Song, H., Huang, L., Zhao, Y., Wang, S., 2021. Comprehensive analysis of differentially expressed lncRNAs miRNAs and mRNA and their ceRNA network of patients with rare-earth pneumoconiosis. Front. Genet. 12, 700398.

Su, L., Nian, Y., Zhu, T., 2023. Circ_PWWP2A promotes lung fibroblast proliferation and fibrosis via the miR-27b-3p/GATA3 axis, thereby aggravating idiopathic pulmonary fibrosis. Acta Biochim. Pol. 70, 525–532.

Wang, Z., Zhang, X., Ji, Y., Zhang, P., Deng, K., Gong, J., Ren, S., Wang, X., Chen, I., Wang, H., Gao, C., Yokota, T., Ang, Y.S., Li, S., Cass, A., Vondriska, T.M., Li, G., Deb, A., Srivastava, D., Yang, H., Xiao, X., Li, H., Wang, Y., 2016. The long noncoding RNA Chaer defines an epigenetic checkpoint in cardiac hypertrophy. Nat. Med. 22, 1131–1139.

Wang, D., Hao, C., Zhang, L., Zhang, J., Liu, S., Li, Y., Qu, Y., Zhao, Y., Huang, R., Wei, J., Yao, W., 2020. Exosomal miR-125a-5p derived from silica-exposed macrophages induces fibroblast transdifferentiation. Ecotoxicol. Environ. Saf. 192, 110253.

Yang, Y., Liu, Y., Chai, Y., Liu, K., Hu, W., Zhao, K., Zhu, Y., Gao, P., Huang, Q., Zhang, C., 2022. Exosomes in pathogenesis, diagnosis, and treatment of pulmonary fibrosis. Front. Pharmacol. 13, 927653.

You, Y., Yuan, H., Min, H., Li, C., Chen, J., 2023. Fibroblast-derived CXCL14 aggravates crystalline silica-induced pulmonary fibrosis by mediating polarization and recruitment of interstitial macrophages. J. Hazard Mater. 460, 132489.

Zhang, H., Zhu, Q., Ji, Y., Wang, M., Zhang, Q., Liu, W., Li, R., Zhang, J., Xu, P., Song, X., Lv, C., 2023. hucMSCs treatment prevents pulmonary fibrosis by reducing circANKRD42-YAP1-mediated mechanical stiffness. Aging (Albany NY) 15, 5514–5534.

Zhou, W., Cai, Z., Liu, J., Wang, D., Ju, H., Xu, R., 2020. Circular RNA: metabolism, functions and interactions with proteins. Mol. Cancer 19, 172.